Vietnam Journal of Catalysis and Adsorption
Tạp chí xúc tác và hấp phụ Việt Nam

https://jca.edu.vn

Isotherm and Kinetic Adsorption Modeling of Methylene Blue on Bio-Based Materials Prepared from *Barringtonia acutangula* Seeds

Thanh-Truc Dang[1,2], Le-Thuy-Thuy-Trang Hoang[3,4], Van-Kieu Nguyen[1,2,*]

[1] *Center for Hi-Tech Development, Nguyen Tat Thanh University, Saigon Hi-Tech Park, Ho Chi Minh City, Vietnam*
[2] *Institute of Interdisciplinary Sciences (IIS), Nguyen Tat Thanh University, Ho Chi Minh City, Vietnam*
[3] *Laboratory of Advanced Materials Chemistry, Institute for Advanced Study in Technology, Ton Duc Thang University, Ho Chi Minh City 72915, Vietnam*
[4] *Faculty of Applied Sciences, Ton Duc Thang University, Ho Chi Minh City 72915, Vietnam*
** Email: kieunv@ntt.edu.vn*

ARTICLE INFO

Received: 07/03/2026
Accepted: 29/03/2026
Published: 30/03/2026

Keywords:
Barringtonia acutangula seeds;
adsorption;
methylene blue;
kinetics;
isotherms

ABSTRACT

The valorization of *Barringtonia acutangula*'s seeds, a common solid waste in Vietnam, as a biosorbent for methylene blue (MB) adsorption was reported. The material's adsorptive properties were evaluated by FTIR, SEM-EDX, and N_2 adsorption-desorption analyzes. Laboratory-scale experiments were conducted, studying the adsorption of MB onto the derived biosorbent under varying adsorption times and initial MB concentrations. Analyzes of the experimental data by kinetic and isotherm models respectively conformed to pseudo-second-order and Langmuir models. The favorable adsorption process by *B. acutangula*'s seed powder was indicated, adapting an adsorption rate of 14.6 mg g^{-1} min^{-1} and a maximum adsorption capacity of 200.0 mg g^{-1}. These findings further substantiate the potential of the prepared biosorbent for MB removal from aqueous environments, and consolidate agricultural by-products or solid waste materials utilization as promising approaches for sustainable and effective wastewater treatment. More in-depth investigation was encouraged, determining this biosorbent applicability in real dye-based wastewater treatment.

Introduction

For years, the escalating demand for textile, apparel, and fashion products have promoted the substantial expansion in dye-intensive industries, such as textile manufacturing, leather processing, tanning, and paint production [1-3]. This development, however, has led to accelerated increase in the release of hazardous effluents, containing synthetic dyes as extremely detrimental contaminants for aquatic environments with high water solubility, low biodegradability, exceptional resistance to chemical, thermal, photolytic degradation [4, 5]. Moreover, the dissemination of dye pollutants into water bodies not only impedes light penetration [6], diminishes dissolved oxygen levels, but also elevates biochemical oxygen demand (BOD) and chemical oxygen demand (COD) [7]. Therefore, deploying appropriate treatment against the contaminated dyes prior to the discharge of dye-based wastewater has been determined as a crucial step to mitigate the aforementioned impacts.

https://doi.org/10.62239/jca.2026.01494

©2025 by the authors. Licensee Vietnam Journal of Catalysis and Adsorption. This article is an open access article distributed under the terms and conditions of the Creative Commons Attribution (CC BY) license (https://creativecommons.org/licenses/by/4.0/).

On this basis, a diverse array of physicochemical treatments has been developed for dye elimination, such as phytoremediation, photodegradation, coagulation-flocculation, advanced oxidation, ion exchange, and adsorption [1, 8-12]. Notably, dyes removal *via* adsorption onto the surface of an adsorbent has been widely recognized as a highly effective technique, advantaged by simple operation, substantial adsorption capacity, cost-effectiveness, efficient regeneration and reusability of the adsorbent, and the absence of secondary pollutant generation [13-16]. In comparison with conventional chemical adsorbents, biosorbents derived from agricultural by-products or solid wastes, such as tamarind fruit peel [17], maize cob [18] or *Artocarpus odoratissimus* stem [19], have garnered significant attention as more economical and more eco-friendly alternatives, not only for dye removal but also for the disposal of these materials. Abundant availability, environmental friendliness, low cost, and commendable performance in dye removal are notable advantages of this approach.

Barringtonia acutangula Gaertn. is a small evergreen plant, widely distributed across east Africa and southeast Asia [20]. Interestingly, to date, no available studies on the potential of *B. acutangula* parts as starting material for biosorbent preparation has been reported. In line with the tendency of utilizing agricultural by-products or solid wastes in new biosorbent preparation, the potential of biosorbent derived from waste seeds of plants [21], and the research gap persisting the usage of *B. acutangula*'s seeds in dye removal, previous study by our research group has successfully utilized this common solid waste as a raw material to prepare a new biosorbent for the removal of MB dye from wastewater [22]. Upon the promising adsorption performance previously reported for *B. acutangula*'s seeds-derived biosorbent, the present study further investigated the MB adsorption process by this material through detailed analyses of both kinetic and isotherm models. These evaluations aim to advance the assessment of this biosorbent potential in practical wastewater treatment application.

Experimental

Chemical

Chemical reagents, including hydrochloric acid 37% (HCl), sodium hydroxide (NaOH), ethanol (96%), and solid methylene blue (MB) dye, were of analytical grade. Distilled water (DW) was used in all experiments. *B. acutangula* seeds were collected in Thu Dau Mot City, Binh Duong Province, Vietnam.

Preparation of BASP

The collected *B. acutangula* seeds were carefully washed with DW to remove the remaining dirt, petal, and pistil. The air-dried seeds (by sunlight) was then applied to the grinding process to acquire BASP, which was preserved at room temperature in airtight and desiccated bags for later experiments.

Material characterization

The adsorptive properties of the acquired BASP were characterized by the following techniques. Fourier transform infrared spectroscopy (FT-IR) within the wavelength range of 4000 – 400 cm^{-1}, recorded by an FT/IR-4X spectrometer (JASCO Inc, Japan), was applied to reveal the functional groups upon the material's surface, while its morphology was evaluated by a S-4800 scanning electron microscope (SEM) (Hitachi, Japan), equipped with an energy dispersive X-ray (EDX) spectrometer (Oxford Instruments). N_2 adsorption-desorption analysis, using a MicroActive for TriStar II Plus, Version 2.03 (Micromeritics Instrument, USA) was performed to determine the material's specific surface area.

Adsorption studies

In accordance with our previous report on the susceptibility of BASP in MB adsorption at varying initial pH and adsorbent doses [22], a chain of one-factor-changed adsorption experiments was conducted to further determine the effect of adsorption time and initial concentration of MB. The detailed experimental conditions were given in Table 1. Each experiment was conducted in triplicate for mean value and standard deviation determination. In each experiment, 0.02 g L^{-1} dose of BASP was added to 40 mL of MB solution with initial pH 8.0, prepared at varying MB concentrations. The adsorption was processed at room temperature for specific time intervals during a 150 rpm agitation. Equilibrium concentrations of the remaining MB in the solution was measured by a V-630 UV-VIS spectrophotometer (Jasco, Japan) at a wavelength of 665 nm. These values were then applied to calculate the adsorption capacity (q_e – mg g^{-1}) *via* Eq. (1) where C_o and C_e (mg L^{-1}) are respectively the initial and equilibrium concentrations of MB, V (L) is the solution volume and M (g) is the adsorbent weight.

$$q_e = \frac{(C_0 - C_e)V}{M} \quad (1)$$

https://doi.org/10.62239/jca.2026.014

Table 1: Investigated factors and experimental conditions in batch adsorption studies

Factors	Studied values	Experimental conditions
Adsorption kinetics	Adsorption time (min) 5, 30, 120, 360, 840, 960	pH: 8.0* BASP dose: 0.02 g L^{-1} MB initial concentration (C_o): 90 mg L^{-1} Room temperature
Adsorption isotherms	MB initial concentration (C_o – mg L^{-1}) 40, 70, 100, 130, 190, 220, 250	pH: 8.0 BASP dose: 0.02 g L^{-1} Adsorption time: 30 h Room temperature

* Adjusted by 0.1 M HCl and 0.1 M NaOH

Results and discussion

Characterization of the BASP

Functional groups of BASP were identified *via* the FT-IR spectrum given in Fig. 1, showing various characterizing vibrational peaks. Accordingly, these included (1) the adsorption bands at 3316 cm^{-1}, assigned to O-H stretching vibration of the -OH groups of the material constituents or of the water adsorbed on its surface [23]; (2) the adsorption peaks at 2937 cm^{-1}, attributed to the stretching vibration of C-H in aliphatic structures [15, 24]; (3) the peak at 1726 cm^{-1} possibly presenting the C=O stretching vibration in carboxyl groups [15]; (4) adsorption peaks at 1618-1426 cm^{-1} and 720 cm^{-1}, respectively characterizing for the stretching vibration of C=C and the bending vibration of C-H in aromatic structures [25, 26] and (5) the adsorption peak at 1074 cm^{-1}, assigned to the stretching vibration of C-O in C-OH [27]. These data suggested the presences of hydroxyl (-OH) and carboxyl (-COOH) groups, as well as aromatic structures in the prepared BASP.

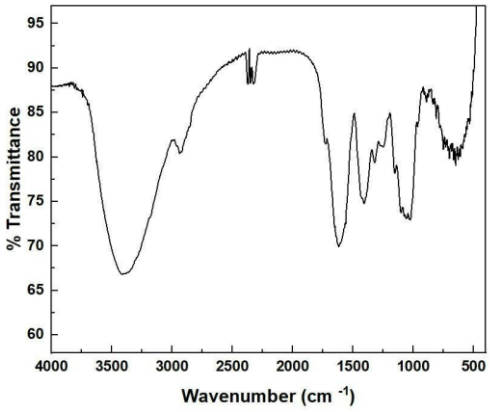

Fig. 1: FT-IR spectrum of the prepared BASP

Consultation on SEM images at varying magnifications displayed the rough amorphous, and irregular surface of BASP (Figs. 2a-2d). EDX analysis further displayed the presence of characteristic peaks corresponding to various elements, notably C, O, and K (Fig. 2e). N_2 adsorption-desorption analysis of the prepared material resulted in a type III isotherm in accordance with IUPAC classification (Fig. 2f), demonstrating the material with apparent non-porous structure. Further application of Brunauer–Emmett–Teller (BET) method provided a humble specific surface area of 4.04 m^2 g^{-1}, which was comparable to other biosorbents from similar starting materials [21] and could be due to the fact that BASP was deployed as a raw biosorbent without prior activation or modification [9, 28].

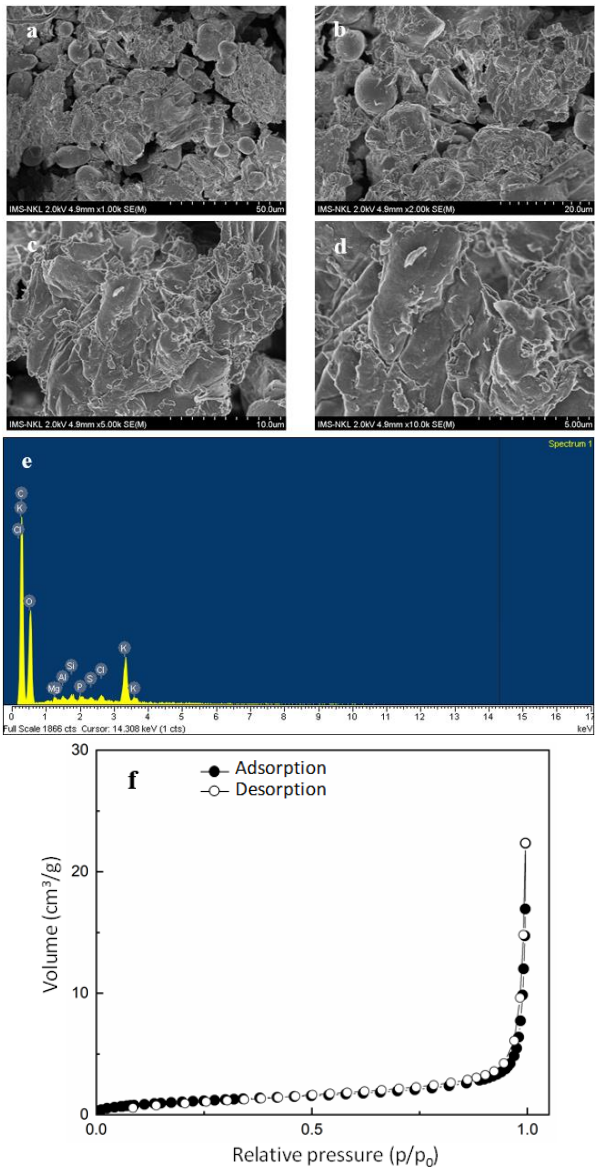

Fig. 2: SEM images at varying magnification (a-d), EDX spectrum (e), and N_2 adsorption-desorption isotherm (f) of BASP.

Adsorption studies

Adsorption kinetics

Following the investigation of the influence of initial pH and adsorbent dose on MB adsorption efficiency using biosorbent from the seeds of *B. acutangula* as reported in our previous study [22], the investigation on adsorption kinetics of the studied BASP (adsorbent)/MB (adsorbate) system was further conducted to determine the adsorption rate and the time interval for the process to attain equilibrium [22, 29, 30].

As demonstrated in Fig. 3a, MB adsorption capacity rapidly enhanced as the adsorption time increased from 5 to 960 minutes, and accomplished equilibrium at 185.5 mg g^{-1} after 360 minutes. These experimental data were subsequently analyzed, adapting two linear kinetics models of pseudo-first-order and pseudo-second-order [31, 32]. The corresponding linear plots, equations, and parameters acquired from the aforementioned models were presented in Figs. 3b-3c and Table 2. Accordingly, experimental kinetic data were best described by pseudo-second-order model, consolidated by the significant regression coefficient (R^2) at 0.999, together with the considerable resemblance to the experimental value of the calculated equilibrium adsorption capacity at 188.7 mg g^{-1}. On this basis, the initial adsorption rate of MB onto the prepared BASP, designated as $h = k_2 q_e^2$, was determined at 29.2 mg g^{-1} min^{-1}.

Table 2. Adsorption kinetic and isotherm parameters for the MB adsorption onto BASP.

Kinetic models	Kinetics model parameters and regression coefficients	
Pseudo-first-order $\log(q_e - q_t) = \log q_e - \frac{k_1}{2.303}t$	k_1 (min^{-1})	0.001
	R^2	0.831
Pseudo-second-order $\frac{t}{q_t} = \frac{1}{k_2 q_e^2} + \frac{1}{q_e}t$	k_2 ($g\ mg^{-1}\ min^{-1}$)	0.0008
	q_e ($mg\ g^{-1}$)	188.7
	R^2	0.999

q_e/q_t ($mg\ g^{-1}$): adsorption capacities at equilibrium/at time t;
k_1 (min^{-1})/k_2 ($g\ mg^{-1}\ min^{-1}$): respective rate constants of kinetics models.

Isotherm models	Isotherm model parameters and regression coefficients	
Langmuir $\frac{C_e}{q_e} = \frac{1}{K_L q_m} + \frac{C_e}{q_m}$	q_m ($mg\ g^{-1}$)	200.0
	K_L ($L\ mg^{-1}$)	0.18
	R^2	0.994
Freundlich $\log q_e = \log K_f + \frac{1}{n}\log C_e$	K_F ($mg\ g^{-1}$)	81.2
	n	5.4
	R^2	0.949

q_e: equilibrium adsorption capacity of adsorbent;
q_m: maximum adsorption capacity of adsorbent;
K_L: Langmuir constant; K_F: Freundlich constant;
C_e: equilibrium concentration of adsorbate.

Adsorption isotherms

The equilibrium adsorption process was further investigated to underscore the influence of MB initial concentration on the adsorption capacity of BASP as depicted in Fig. 3d. Accordingly, the rise in initial MB concentration also resulted in a progressive increase in adsorption capacity. In the same manner to adsorption kinetics study, two linear isotherm models, namely Langmuir [33] and Freundlich [34], were adapted to further analyze the obtained experimental data.

According to the corresponding linear plots and the acquired parameters presented in Figs. 3e-3f and Table 2, the best fit of the experimental equilibrium data to the Langmuir model was exhibited and clearly validated by the significant regression coefficient (R^2) at 0.994. On this basis, the maximum adsorption capacity (q_m) for BASP was determined at 200 mg g^{-1}, which is comparable to biosorbents from other plant materials as enlisted in Table 3. Additionally, further analysis of dimensionless constant (R_L), a characteristic parameter in Langmuir model calculated by Eq. (2), was processed to provide a glance over the nature of MB adsorption upon BASP. Accordingly, based on R_L value, the adsorption process can be deemed unfavorable, irreversible or linear as $R_L > 1$, $0 < R_L < 1$, or $R_L = 1$, respectively [35, 36]. Regarding the deployed initial MB concentrations, the corresponding R_L values were calculated in the range of 0.02 – 0.12, indicating that adsorption of MB on the surface of BASP is favorable.

$$R_L = \frac{1}{1 + K_L C_0} \quad (2)$$

Correlating the material characterization with the adsorption behavior provides insight into the nature of methylene blue (MB) uptake onto BASP. FT-IR spectrum confirmed the presence of hydroxyl and carboxyl functional groups on BASP's surface, which serve as key active sites for MB adsorption. These oxygen-containing groups can readily undergo electrostatic interactions or hydrogen bonding with the cationic dye MB. Additionally, the presence of aromatic C=C and C–H structures suggested possible π–π interactions between the aromatic rings of MB and the carbonaceous matrix of BASP. The surface morphology and textural properties further supported the observed adsorption mechanism. SEM images revealed an irregular and rough surface, providing accessible binding sites despite the absence of a developed porous structure. The non-porous nature of BASP was confirmed by the type III N_2 adsorption-desorption isotherm and the relatively low BET surface area of 4.04 $m^2\ g^{-1}$. However, the material exhibited notable

https://doi.org/10.62239/jca.2026.014

MB adsorption capacity, indicating that chemisorption, rather than physical adsorption or pore filling, dominates the adsorption process. This was consistent with the pseudo-second-order kinetic model, which assumes that the rate-limiting step involves chemical interactions between MB and the active surface sites. Furthermore, the good fit to the Langmuir isotherm model suggested monolayer coverage, which aligns with the presence of specific functional groups acting as adsorption centers.

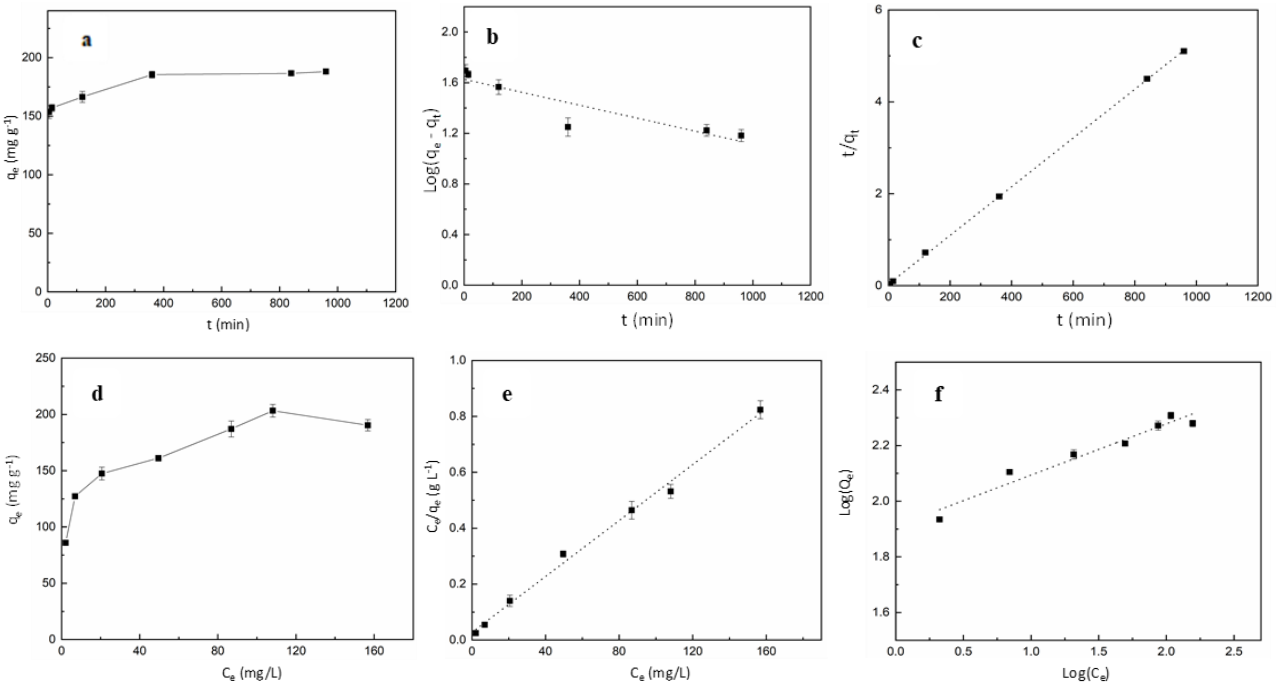

Fig. 3: Adsorption kinetics on BASP (a), pseudo-first order model linear plot (b), pseudo-second order model linear plot (c); Isotherm of MB adsorption on BASP (d), Langmuir isotherm model (e), Freundlich isotherm model linear plot (f) for MB adsorption onto BASP.

Table 3. Comparison of maximum adsorption capacity (q_m) of BASP with different adsorbents for MB removal.

Adsorbents	q_m (mg g^{-1})	Ref
Hazelnut shells	59.17	[37]
Neem leaf powder	8.76	[38]
Yellow passion fruit waste	44.7	[39]
Garlic peel	82.64	[40]
Annona glabra seeds powder	98.0	[21]
Mango seed kernel powder	142.86	[41]
Garlic straw	256.41	[42]
Velvet tamarind fruit shell powder, modified with HCl	63.87	[43]
Ball-milled biochar	354.4	[44]
Modified lychee seed biochar	124.5	[45]
B. acutangula seeds powder	200.0	This study

Conclusion

Herein, a biosorbent from *B. acutangula* seeds were prepared, characterized by rough and irregular surface, and the presence of aromatic structures, hydroxyl and carbonyl groups. The adsorption capacity of the material toward MB dyes in aqueous media was investigated under varying adsorption times and initial MB concentrations. Kinetic analysis revealed that the adsorption of MB onto the *B. acutangula* seeds-derived biosorbent followed a pseudo-second-order kinetic model, with the determined initial adsorption

https://doi.org/10.62239/jca.2026.014

rate of 14.6 mg g^{-1} min^{-1}. Isotherm studies demonstrated the excellent conformity to the Langmuir isotherm model of the adsorption process which was deemed favorable and exhibited a maximum adsorption capacity of 200.0 mg g^{-1}. Collectively, the detailed evaluation of both kinetic and isotherm models confirms the susceptibility of *B. acutangula* seeds powder in MB dyes removal, and therefore encouraging further investigations on the application of this biosorbent in real dye-based wastewater treatment. These findings highlight the potential of utilizing agricultural by-products or solid waste materials in wastewater treatment processes, thereby contributing to resource recycling and the protection of water resources.

Competing Interests

The authors have no relevant financial or non-financial interests to declare.

Data Availability

The data that support the findings of this study are included within the article.

Acknowledgements

We acknowledge Nguyen Tat Thanh University, Ho Chi Minh City, Vietnam for supporting this study.

References

1. D. Nayeri, S.A. Mousavi, J. Environ. Health Sci. Eng., 18(2) (2020) 1671-1689. https://doi.org/10.1007/s40201-020-00566-w
2. M.T. Dao, V.C.N. Nguyen, T.N. Tran, X.D. Nguyen, D.T. Vo, V.K. Nguyen, L.T.T.T. Hoang, J. Chem., 2021 (2021) 7608856. https://doi.org/10.1155/2021/7608856
3. R. Rehman, S. Majeed, Int. J. Phytoremediat., 24(10) (2022) 1004-1013. https://doi.org/10.1080/15226514.2021.1991269
4. F. Mashkoor, A. Nasar, Inamuddin, A.M. Asiri, Sci. Rep., 8 (2018) 8232. https://doi.org/10.1038/s41598-018-26655-3
5. L.R. Oviedo, V.R. Oviedo, L.D. Dalla Nora, W.L. da Silva, Sep. Purif. Technol., 315 (2023) 123712. https://doi.org/10.1016/j.seppur.2023.123712
6. M.T. Yagub, T.K. Sen, M. Ang, Environ. Earth Sci., 71(4) (2014) 1507-1519. https://doi.org/10.1007/s12665-013-2555-0
7. S. Samsami, M. Mohamadizaniani, M.H. Sarrafzadeh, E.R. Rene, M. Firoozbahr, Process Saf. Environ. Prot., 143 (2020) 138-163. https://doi.org/10.1016/j.psep.2020.05.034
8. V.V. Chandanshive, S.K. Kadam, R.V. Khandare, M.B. Kurade, B.H. Jeon, J.P. Jadhav, S.P. Govindwar, Chemosphere, 210 (2018) 968-976. https://doi.org/10.1016/j.chemosphere.2018.07.064
9. T.M. Dao, T.T. Luu, Bioresour. Technol. Rep., 12 (2020) 100583. https://doi.org/10.1016/j.biteb.2020.100583
10. U.B. Deshannavar, P.K. Singa, D. Gaonkar, A. Gayathri, A. Patil, L.V. Malade, Mater. Today Proc., 24 (2020) 1011-1019. https://doi.org/10.1016/j.matpr.2020.04.414
11. T. Shindhal, P. Rakholiya, S. Varjani, A. Pandey, H.H. Ngo, W. Guo, H.Y. Ng, M.J. Taherzadeh, Bioengineered, 12(1) (2021) 70-87. https://doi.org/10.1080/21655979.2020.1863034
12. H.M. Solayman, M.A. Hossen, A.A. Aziz, N.Y. Yahya, K.H. Leong, L.C. Sim, M.U. Monir, K.D. Zoh, J. Environ. Chem. Eng., 11(3) (2023) 109610. https://doi.org/10.1016/j.jece.2023.109610
13. B. Kakavandi, A. Raofi, S.M. Peyghambarzadeh, B. Ramavandi, M.H. Niri, M. Ahmadi, Desalin. Water Treat., 111 (2018) 310-321. https://doi.org/10.5004/dwt.2018.22238
14. G. Gopal, S.A. Alex, N. Chandrasekaran, A. Mukherjee, RSC Adv., 10(45) (2020) 27081-27095. https://doi.org/10.1039/D0RA04264A
15. V.S. Munagapati, H.Y. Wen, Y. Vijaya, J.C. Wen, J.H. Wen, Z. Tian, G.M. Reddy, Raul, J. Garcia, Int. J. Phytoremediat., 23(9) (2021) 911-923. https://doi.org/10.1080/15226514.2020.1866491
16. D. Naghipour, L. Hoseinzadeh, K. Taghavi, J. Jaafari, A. Amouei, Int. J. Environ. Anal. Chem., 103(12) (2023) 5706-5719. https://doi.org/10.1080/03067319.2021.1942462
17. M.S. Reddy, Dyes Pigm., 74(3) (2007) 727-735. https://doi.org/10.1016/j.dyepig.2006.06.009
18. G.H. Sonawane, V.S. Shrivastava, Desalination, 247(1-3) (2009) 430-441. https://doi.org/10.1016/j.desal.2009.01.006
19. A. Saeed, M. Sharif, M. Iqbal, J. Hazard. Mater., 179(1-3) (2010) 564-572. https://doi.org/10.1016/j.jhazmat.2010.03.041
20. A.S. Ahmad, T. Sae-Leaw, B. Zhang, S. Benjakul, Food Control, 155 (2024) 110037. https://doi.org/10.1016/j.foodcont.2023.110037
21. L.T.T.T. Hoang, H.V.T. Phan, P.N. Nguyen, T.T. Dang, T.N. Tran, D.T. Vo, V.K. Nguyen, M.T. Dao, Arch. Environ. Contam. Toxicol., 86(1) (2024) 48-57. https://doi.org/10.1007/s00244-023-01044-8

22. T.T. Dang, T.T. Duyen, H.L.T.T. Trang, Nat. Resour. Environ. Mag., 9(407) (2023) 46-47.
23. J. Georgin, K. da Boit Martinello, D.S. Franco, M.S. Netto, D.G. Piccilli, M. Yilmaz, L.F. Silva, G.L. Dotto, J. Environ. Chem. Eng., 10(1) (2022) 107006. https://doi.org/10.1016/j.jece.2021.107006
24. H.A. Pawar, K.G. Lalitha, Int. J. Biol. Macromol., 65 (2014) 167-175. https://doi.org/10.1016/j.ijbiomac.2014.01.026
25. V. Sharma, S. Bhardwaj, R. Kumar, Vib. Spectrosc., 101 (2019) 81-91. https://doi.org/10.1016/j.vibspec.2019.02.006
26. M. Agarwal, V.K. Kudapa, J. Sudharsan, Mater. Today Proc., 47 (2021) 5319-5325. https://doi.org/10.1016/j.matpr.2021.06.055
27. P. Arulmathi, C. Jeyaprabha, P. Sivasankar, V. Rajkumar, Clean (Weinh)., 47(7) (2019) 1800464. https://doi.org/10.1002/clen.201800464
28. N. Abbasi, S.A. Khan, T.A. Khan, J. Water Process Eng., 43 (2021) 102267. https://doi.org/10.1016/j.jwpe.2021.102267
29. M.T. Dao, T.P.L. Tran, D.T. Vo, V.K. Nguyen, L.T.T.T. Hoang, Adv. Mater. Sci. Eng., 2021 (2021) 2543197. https://doi.org/10.1155/2021/2543197
30. V.G. Georgieva, L. Gonsalvesh, M.P. Tavlieva, J. Mol. Liq., 312 (2020) 112788. https://doi.org/10.1016/j.molliq.2020.112788
31. T.T.T.L. Hoang, F. Unob, S. Suvokhiaw, N. Sukpirom, J. Environ. Chem. Eng., 8(2) (2020) 103653. https://doi.org/10.1016/j.jece.2020.103653
32. A. Das, N. Bar, S. Das, J. Colloid Interface Sci., 580 (2020) 245-255. https://doi.org/10.1016/j.jcis.2020.07.017
33. I. Langmuir, J. Am. Chem. Soc., 38(11) (1916) 2221-2295. https://doi.org/10.1021/ja02268a002
34. H. Freundlich, Z. Phys. Chem., 57(1) (1907) 385-470. https://doi.org/10.1515/zpch-1907-5723
35. A. Dada, A. Olalekan, A. Olatunya, O. Dada, IOSR J. Appl. Chem., 3(1) (2012) 38-45. https://doi.org/10.9790/5736-0313845
36. J.W.P. Lye, N. Saman, S.S.N. Sharuddin, N.S. Othman, S.S. Mohtar, A.M. Md Noor, J. Buhari, S.C. Cheu, H. Kong, H. Mat, Clean (Weinh)., 45(10) (2017) 1600260. https://doi.org/10.1002/clen.201600260
37. F. Ferrero, J. Hazard. Mater., 142(1-2) (2007) 144-152. https://doi.org/10.1016/j.jhazmat.2006.07.072
38. K.G. Bhattacharyya, A. Sharma, Dyes Pigm., 65(1) (2005) 51-59. https://doi.org/10.1016/j.dyepig.2004.06.016
39. F.A. Pavan, E.C. Lima, S.L.P. Dias, A.C. Mazzocato, J. Hazard. Mater., 150(3) (2008) 703-712. https://doi.org/10.1016/j.jhazmat.2007.05.023
40. B. Hameed, A. Ahmad, J. Hazard. Mater., 164(2-3) (2009) 870-875. https://doi.org/10.1016/j.jhazmat.2008.08.084
41. K.V. Kumar, A. Kumaran, Biochem. Eng. J., 27(1) (2005) 83-93. https://doi.org/10.1016/j.bej.2005.08.004
42. F. Kallel, F. Chaari, F. Bouaziz, F. Bettaieb, R. Ghorbel, S.E. Chaabouni, J. Mol. Liq., 219 (2016) 279-288. https://doi.org/10.1016/j.molliq.2016.03.024
43. M.A. Khoj, L.S. Almazroai, Biomass Convers. Biorefin., 14(20) (2024) 23841-23855. https://doi.org/10.1007/s13399-023-04419-y
44. H. Lyu, B. Gao, F. He, A.R. Zimmerman, C. Ding, J. Tang, J.C. Crittenden, Chem. Eng. J., 335 (2018) 110-119. https://doi.org/10.1016/j.cej.2017.10.130
45. S. Sahu, S. Pahi, S. Tripathy, S.K. Singh, A. Behera, U.K. Sahu, R.K. Patel, J. Mol. Liq., 315 (2020) 113743. https://doi.org/10.1016/j.molliq.2020.113743